



PERFORMANCE ANALYSIS OF DUAL BAND BANDPASS FILTER DESIGN TECHNOLOGIES

KM Vandana

Department of Electronics Communication, HR Institute of Technology, Merta Duhai Ghaziabad, Ghaziabad, Uttar Pradesh

ABSTRACT

This paper focuses on different design techniques of dual band band-pass filter and their results are compared. Improvement of filter performance and reduction in components size is become prime concern with rapid advancement of technologies. In this paper, Coupled Stepped Impedance Resonators, Series Coupled Ring Resonator, Single Ring Resonator and Stub-Loaded Meander Line Resonator.

INTRODUCTION

These days, there is an extraordinary interest for multiband and multimode transceivers with the end goal that diverse wireless gauges coincide and permit worldwide use. For instance, a GSM-CDMA handset must have the option to get and transmit signals at 900 MHz and 1900 MHz [1, 2]. To obtain this multi-usefulness, one can utilize separate chips for every standard, which implies that everyone must be independently planned, tried and stuffed and, along these lines, a costly arrangement. The profoundly attractive arrangement depends on equipment reuse. In this unique circumstance, we present a double band structure system for one of the RF front-end obstructs the pass-band channel. Different dual-band band-pass filters have been introduced, [3-5].

Double band bandpass channels (DBBPF) have as of late become appealing parts in wireless correspondence frameworks [6-13]. In [6] the DBBPF is accomplished by combining two individual single-band channels by means of a common input/output port. This sort of DBBPF is anything but difficult to acknowledge, in light of the fact that the sign of the two bands go through various resonators, allowing the two individual single band channels to be designed independently. Be that as it may, this sort of channel

requires in any event four resonators, on the grounds that a single-band channel design requires multiple resonators. In [7-9], a double mode resonator, which has a controllable first harmonic resonant frequency, is utilized to make the second passband. This kind of DBBPF can just determine the focal frequencies of two passbands. They experience issues in regulating the bandwidths of the two passbands in request to accomplish different particulars for each passband. DBBPFs with controllable bandwidths have been examined [10-13]. Nonetheless, these channels have constrained controllable bandwidth resulting from the common coupling way and require a complex design methodology. In this paper, diverse design systems for double band-pass channel is contrasted with break down their presentation.

LITERATURE SURVEY

He Zhu and Amin M. Abbosh [14] proposed new sort of stepped-impedance resonator with embedded coupled-line section. Contrasted and the creators' design [15] where a double band channel was designed using multi-mode resonators, the new channel utilizes a couple of coupled stepped-impedance resonator with embedded coupled-line for both of single-and double band channel designs. The investigation of the proposed resonator is firstly introduced, and afterward



two BPFs (a single-band and a double band model) are assembled and tried for confirmation of the design approach.

N. A. Wahab[16] displayed a novel ring based topology which utilizes just one quarter-wavelength coupled-line. This design proposed two rings cascaded in series side by side, coupled by means of a single quarter-wavelength coupled-line to display double band double mode bandpass channel. By using just one coupled-line and two identical rings had diminished the quantity of controlled parameters along these lines rearranges the tuning procedure. Adding to this, the pseudo-elliptic attributes of the two rings will improve the selectivity of the double band channel since transmission zeros are shaped both at the lower and upper stopbands of the double band. Further examination on the channel bandwidth, passband reaction and out-of-band reaction are additionally displayed by controlling the channel components of line impedances, Z_r , odd-and even-mode impedances of the coupled-line, Z_{oo} and Z_{oe} separately reaction.

ShaLuo [17] centers around a novel double mode double band BPF with two transmission shafts in two passbands is designed dependent on a single microstrip ring resonator on a single-layer substrate. The two energized ports are put along the ring with a partition of 135 and they are capacitively coupled to this ring through parallel-coupled lines. The remaining pieces of this work depict the principle of the proposed ring resonator double band channel and show its double band execution through an equal circuit model. Finally, a reduced double BPF with occasionally loading of opened stubs is designed for 2.4/5.8 GHz wireless local area network applications, and the anticipated outcomes are affirmed tentatively.

Naoto Sekiya[18] introduced a minimized high-temperature superconductor (HTS) double band bandpass channels by using stub-stacked wander open-circle resonator. Specifically, they depict the new technique for deftly adjusting the coupling coefficient for two bands. Use of the double band bandpass channels to a tri-band bandpass channels was portrayed with simulation.

DUAL BAND BANDPASS FILTER DESIGNING TECHNIQUES

A pair of coupled stepped-impedance resonators and its use to build single- and dual-band bandpass filter (BPF) is shown in fig. 1.

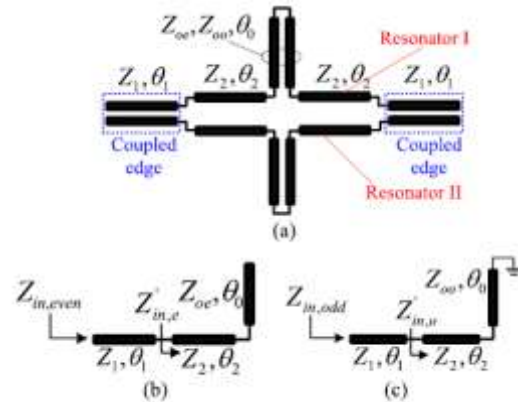


Fig. 1 (a) coupled stepped-impedance resonators (b) even- and (c) odd-mode equivalent circuits

This design includes a pair of coupled stepped-impedance resonators with embedded coupled-line sections. The utilized resonator is composed of two stepped-impedance transmission lines (Z_1, Z_2, θ_1 , and θ_2) and an embedded coupled-line section (Z_{oe}, Z_{oo}, θ_0). The overall length of the structure is about half guided-wavelength ($\lambda_g/2$) at the center frequency f_0 . The proposed resonator is asymmetric, and thus, odd- and even-analysis methods can be adopted to analyze its structure and deduce its resonant frequencies. Fig. 1(b) and (c) show the even- and odd-mode equivalent circuits, which can be used to derive the resonant frequencies. For the even-mode case, the resultant input impedance can be expressed as

$$Z_{in,even} = Z_1 \frac{Z'_{in,e} + jZ_1 \tan \theta_1}{Z_1 + jZ'_{in,e} \tan \theta_1}$$

$$Z'_{in,e} = jZ_2 \frac{Z_2 \tan \theta_2 - Z_{oe} \tan \theta_0}{Z_2 + Z_{oe} \tan \theta_2 \tan \theta_0}$$

The even-mode resonant frequencies can be determined by setting $Z_{in,even} = 0$. Here the first three even-modes (f_{e1}, f_{e2} , and f_{e3}) are investigated. For odd-mode case, the resultant input impedance can be expressed as

$$Z_{in,odd} = Z_1 \frac{Z'_{in,o} + jZ_1 \tan \theta_1}{Z_1 + jZ'_{in,o} \tan \theta_1}$$

$$Z'_{in,o} = jZ_2 \frac{Z_2 \tan \theta_2 + Z_{oo} \tan \theta_0}{Z_2 - Z_{oo} \tan \theta_2 \tan \theta_0}$$

The odd-mode resonant frequencies can be determined by setting $Z_{in,odd} = 0$. Here, the first three odd-modes (f_{o1}, f_{o2} , and f_{o3}) are investigated. This filter is a second-order structure composed of two resonators. The



coupling between the two resonators is realized by the open-ended transmission line (Z_1 and θ_1), as marked as coupling edges in Fig. 1(a). The electrical length (at the center frequency of the first passband f_1) of the stepped impedance and coupled-line section should meet the equation

$$2(\theta_1 + \theta_2) + \theta_0 = 180^\circ.$$

For different kinds of filter types (single- or dual-band), the following relation should be satisfied to find the values of θ_0, θ_1 , and θ_2 based on extensive parametric studies:

$$\begin{cases} \theta_1 = 2\theta_0 & \text{single-band} \\ \theta_1 = \theta_0 & \text{dual-band.} \end{cases}$$

Equation (6) defines the conditions of exciting or highly suppressing the first even-mode resonant frequency f_{e1} .

A **dual-band ring filter** using two identical microstrip dual-mode ring resonators shown in Fig. 2 (a), two identical rings are coupled in series with a single quarter-wavelength coupled-line at the center of the structure to form a dual-band bandpass filter. The input and output power of the resonator is fed via the ring lines which created a dual-path effect. The basic cell having one wavelength long at frequency f_0 with a coupled-line produced a dual-mode response with two transmission zeros. It is also known that a quarter-wavelength coupled-line behaves as a bandstop filter. Hence, by having a four-port coupled-line at the center of the structure has helped to create isolation between the two passbands resulting to a center transmission zero.

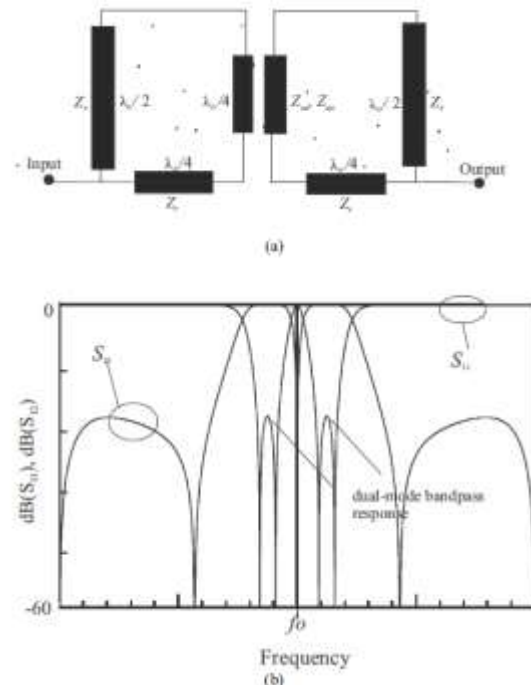


Fig.2 (a) A proposed dual-band ring filter topology, (b) Ideal response of the dual-band [16]

A set of impedance values of the ring resonators are chosen to obtain an ideal response of the bandpass filter, i.e. $Z_r = 50 \Omega$, $Z_{oe} = 243 \Omega$ and $Z_{oo} = 74 \Omega$ for reference frequency, f_0 at 2 GHz. Fig. 2(b) demonstrates the dual-mode dual-band response with sharp rejection skirt and center transmission zero at f_0 to isolate the two passbands.

Further investigation to analyze the filter behavior is performed. Figs. 3, 4, and 5 illustrate the characteristics of the bandpass filter with center frequency, f_0 at 2 GHz. The filter elements of Z_r , Z_{oe} and Z_{oo} are investigated to analyze their influence as the controlling parameters on the responses of the dual-band filter. The investigation is conducted by varying one of the controlling parameters while the other two impedances are fixed.

Figs. 3 and 4 illustrate the bandwidth variations when Z_r or Z_{oe} is varied. Fig. 3 demonstrates the effect of Z_r , in which when the impedance is increased while fixing both Z_{oe} and Z_{oo} , the bandwidth is decreased. Whereas when the impedance Z_{oe} is increased and Z_r and Z_{oo} are fixed, the bandwidth will be increased.

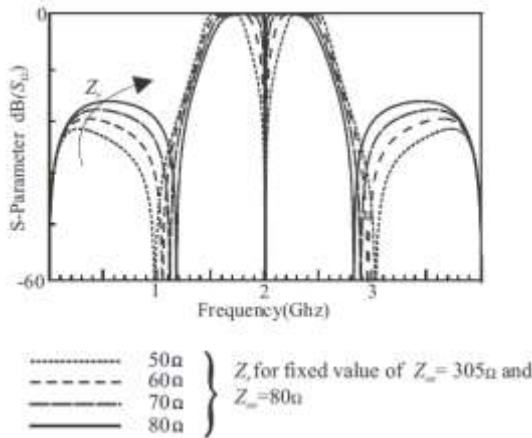


Fig. 3 Variations of bandwidth and rejection level when Z_r is varied while Z_{oe} and Z_{oo} are fixed

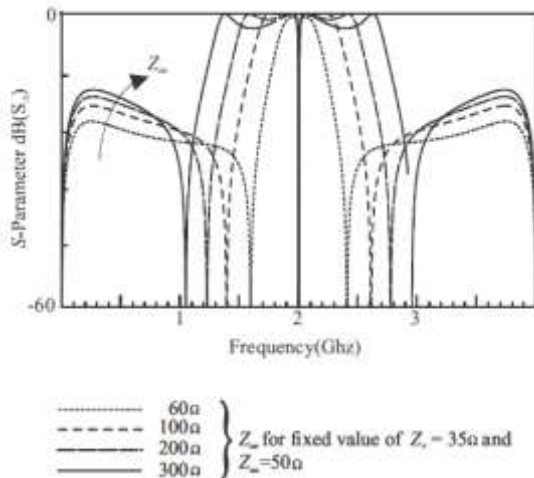


Fig. 4 Variations of bandwidth when Z_{oe} is varied while Z_r and Z_{oo} are fixed

Next, when Z_{oo} is varied, and both Z_r and Z_{oe} are fixed, the insertion loss and rejection level will be affected. Fig. 5 illustrates the outcome of varying Z_{oo} while the other two parameters are fixed. Meanwhile, by increasing Z_{oo} , the insertion loss deteriorates but the rejection level will be improved.

These observations had demonstrated that to achieve desired response, all the three parameters i.e. Z_r , Z_{oe} and Z_{oo} must be tuned to achieve desired bandwidth, insertion loss and rejection level. Therefore, the filter elements that influenced the overall response of this design is contributed by the line impedance of the two rings, Z_r and the single quarter wavelength coupled-line impedances, Z_{oe} and Z_{oo} respectively.

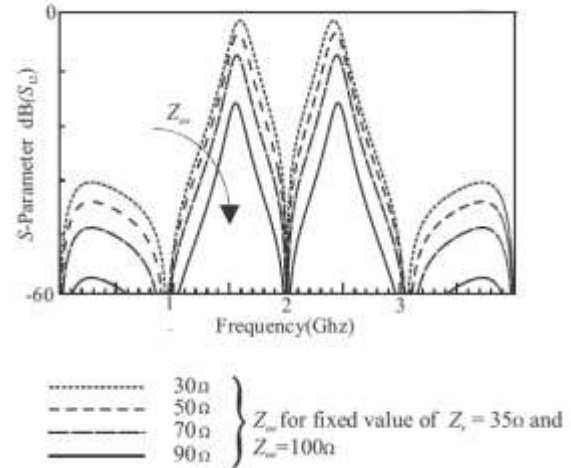


Fig. 5 Variations of passband and insertion loss when Z_{oo} is varied while Z_{oe} and Z_r are fixed

Fig. 6(a) depicts the schematic of the proposed dual-mode dual-band microstrip ring resonator, where is the input and output port impedance, and are the inner and outer radii of this ring, and is the characteristic impedance of the ring. In our design, the parallel-coupled lines are one quarter of the length of the ring, with a width of w and a spacing of s . As illustrated in Fig. 6(a), a three-port parallel-coupled line can be treated as a capacitive impedance, a voltage transformer with turns ratio and two parallel-connected lines at port 2 and 3 as discussed in [19]. and denote the even and odd-mode characteristic impedances of this parallel-coupled line, while is their effective electrical length.

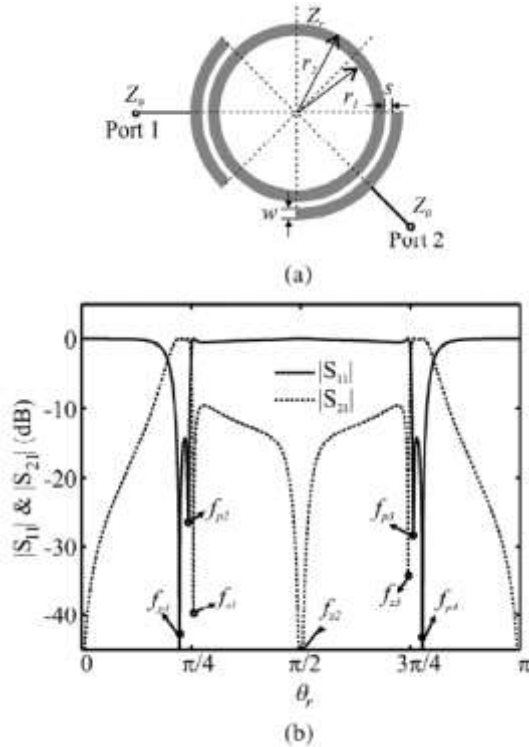


Fig. 6 Proposed dual-mode dual-band BPF using a single uniform ring resonator. (a) Schematic. (b) S-parameters versus electrical length θ_r with θ_r and θ_r .

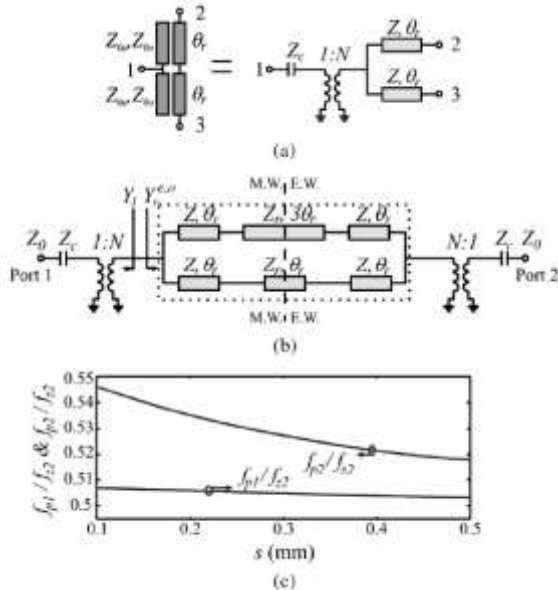


Fig. 7 (a) Equivalent-circuit diagram of three-port parallel-coupled lines. (b) Complete equivalent-circuit model for the filter in Fig. 1(a). (c)

Normalized frequencies of the two poles (f_{p1} and f_{p2}) in the first passband versus spacing s with s and s . Substrate: ϵ_r and μ_r .

Follow the work in [20], the relationship between all the element parameters of the two networks in Fig. 7(a) can be derived as

$$Z_c = -j \frac{Z_{0e} Z_{0o}}{\tan \theta_r (Z_{0e} + Z_{0o})}$$

$$N = \frac{Z_{0e} + Z_{0o}}{Z_{0e} - Z_{0o}}$$

As such, the equivalent-circuit model of the filter in Fig. 6(a) can be derived as shown in Fig. 7(b). Fig. 6(b) plots its simulated parameters versus electrical length. As can be observed, the first and second passbands with two transmission poles at each band appear at f_{p1} and f_{p2} , respectively.

The two lower ones (f_{p1} and f_{p2}) are symmetrically located at the low sides of the two higher ones (f_{s1} and f_{s2}) with respect to $\theta_r = \pi/2$. In addition, there exist three transmission zeros, f_{z1} , f_{z2} , and f_{z3} , between the two passbands. We can analyze this proposed ring resonator filter based on Fig. 7(b). According to the transmission theory, transmission zeros of this ring filter occur at the frequencies where the overall mutual admittance of the network inside the dash square in Fig. 7(b) equals to 0, such that

$$Z \sin 2\theta_r (\cos \theta_r + \cos 3\theta_r) + A (\sin \theta_r + \sin 3\theta_r) = 0$$

where $A = \frac{Z_{0e} Z_{0o}}{Z_{0e} - Z_{0o}}$ and $Z = \frac{Z_{0e} + Z_{0o}}{Z_{0e} - Z_{0o}}$.

By solving (2), all the zeros can be determined as

$$\theta_r = \sin^{-1} \sqrt{\frac{Z_r}{Z + Z_r}}$$

$$\theta_r = \left(n + \frac{1}{2} \right) \pi.$$

Equation (3a) determines the first and third transmission zeros, and while the second zero, f_{z2} , is derived under in (3b).

Stub-loaded resonators, which have an easily controlled resonant frequency, have been applied to normal conductor DBPFs. They have two resonance



modes of even and oddmodes. The even-mode resonant frequency can be easily tunedwhile keeping the odd-mode one basically the same. However,it is difficult to keep the even-mode one basically the samewhile tuning the odd-mode one. Therefore, we proposed a noveldual-band bandpass stub-loaded resonator which can be independentlycontrolled of the resonant frequency of the even andodd modes.

Fig. 8(a) shows the configuration of the double band bandpass stub-stacked resonator we created. It comprises of a meander open-loop resonator and an open stub. The meander resonator is utilized for miniaturizing the double band resonator size as well as decreasing the space between resonators because of feeble coupling property. This symmetric configuration empowers investigation as far as even-and odd-mode excitation's (the An A_ plane carries on as an electric/magnetic wall for odd/even excitation). Fig. 8(b) and (c) show the odd-mode excitation and even-mode excitation.

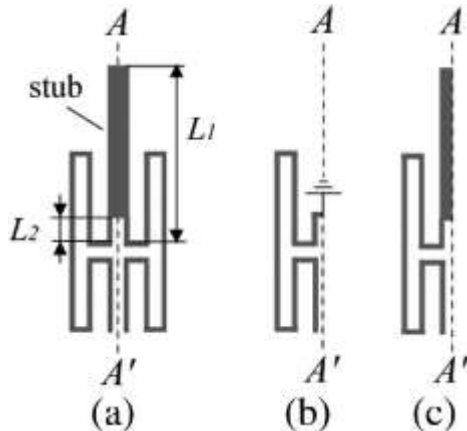


Fig. 8 (a) Configuration of proposed dual-band resonator, (b) odd-mode, and(c) even-mode excitation

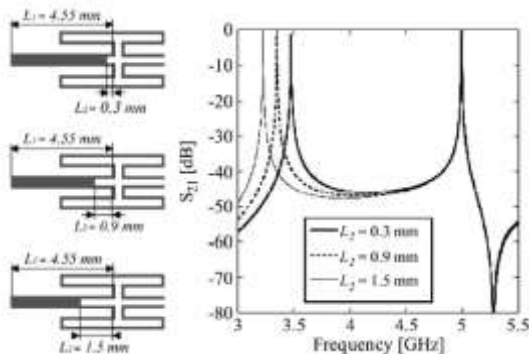


Fig. 9 Configuration of proposed resonator with length L2 of 0.3, 0.9,1.5 mm and simulated resonant frequency responses for different values of L2.

For odd-mode excitation, there is a voltage null along themiddle of the resonator, as shown in Fig. 8(b). Hence, the tappingpoint of the stub is actually a virtual ground for theodd-mode. As a consequence, the stub does not affect the odd moderesonant frequency. For even-mode excitation, there is nocurrent flow through the symmetrical plane. Thus, we can bisectthe circuit with open circuits at the A-A_ plane, so that an even moderesonator which is constructed with meander line and theopen stub is obtained, as shown in Fig. 8(c).

To investigate the frequency response of the developed resonator,we used full-wave simulation using electromagnetic(EM) analysis software (Sonnet EM) based on the momentmethod [21].The odd-mode resonant frequency was mainly determined bythe length of the meander open-loop resonator as in Fig. 8(b).The configuration of the proposed resonator for three values oflength L2, and the simulated resonant frequency responses forthe three values are plotted in Fig. 2. Increasing L2 from 0.3to 1.5 mm effectively shifted the odd-mode resonant frequency250 MHz while leaving the even-mode resonant frequencybasically the same. This is because the electrical length of even moderesonance was not changed, as shown in Fig. 9, and thestub does not affect the odd-mode resonant frequency.

The even-mode resonant frequency is mainly determined bythe total length of the meander open-loop resonator and stubsee Fig. 8(c). The configuration of the proposed resonator forthree values of length L1, and the simulated resonant frequencyresponses for the three values are plotted in Fig. 10 Reducing L1from 4.55 to 3.55 mm without changing L2 effectively shiftedthe even-mode resonant frequency 407 MHz while leavingthe odd-mode resonant frequency basically the same. This is

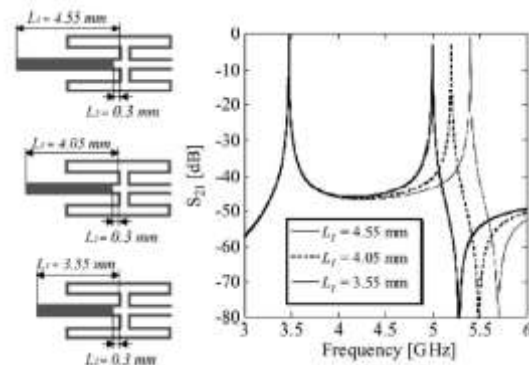




Fig. 10 Configuration of proposed resonator with length $L1$ of 4.55, 4.05, 3.55 mm and simulated resonant frequency response for different values of $L1$ because the electrical length of odd-mode resonance was not changed, as shown in Fig. 10, and the stub does not affect the odd-mode resonant frequency.

CONCLUSION

There are several methods available to design a filter. In this paper some of the methods are discussed and compared along with the results and advantages. Compatibility of methods may differ according to the desired filter specification required for the particular use. Discussed filtering techniques led to the evolution of the number of filters. These filters have been used in a wide range of applications.

REFERENCES

1. C. Y. Chen, C. Y. Hsu and H. R. Chuong, "Design of Miniature Planar Dual Band Filter Using Dual-Feeding Structures and Embedded Resonators," *IEEE Microwave and Wireless Components Letters*, Vol. 16, No. 12, 2006, pp. 669-671. doi:10.1109/LMWC.2006.885621
2. S. F. Chang, Y. H. Jeng and J. L. Chen, "Dual-Band Step Impedance Band Pass Filter for Multimode Wireless LANs," *Electronic Letters*, Vol. 40, No. 1, 2004, pp. 38-39. doi:10.1049/el:20040065
3. H. Miyake, S. Kitazawa, T. Ishizaki, T. Ymada and Y. Nagatomi, "A Miniaturized Monolithic Dual-band Filter Using Ceramic Lamination Technique for Dual Mode Portable Telephones," *IEEE MTT-S International Microwave Symposium Digest*, 8-13 June 1997, Vol. 2, pp. 789-792.
4. J. T. Kuo, T. H. Yeh and C. Yeh, "Design of Microstrip Bandpass Filters with a Dual Pass Band Response," *IEEE Microwave Theory and Techniques Transactions*, Vol. 53, No. 4, April 2005, pp. 1331-1337. doi:10.1109/TMTT.2005.845765
5. X. Y. Zhang, J. X. Chen and Q. Xue, "Dual-band Band Pass Filters Using Stub-Loaded Resonators," *IEEE Microwave and Wireless Components Letters*, Vol. 17, No. 8, 2007, pp. 583-585. doi:10.1109/LMWC.2007.901768
6. C. -Y. Chen, C. -Y. Hsu, "A simple and effective method for microstrip dual-band filters design," *IEEE Microwave and Wireless Component Letters*, vol. 16, no. 5, pp. 246-248, May 2006.
7. S. Gao, Z. -Y. Xiao, and W. -F. Chen, "Dual-band bandpass filter with source-load coupling," *Electronics Letters*, vol. 45, no. 17, pp. 894-895, Aug. 2009.
8. J. Lee, J. Jung, K. Kim, and Y. Lim, "Compact dual-mode interdigital-loop resonator and filter application," *Wireless Information Technology and Systems 2010*, pp. 1-4, 2010.
9. P. Mondal, M. -K. Mandal, "Design of dual-band bandpass filters using stub-loaded open-loop resonators," *IEEE Transactions Microwave Theory and Techniques*, vol. 56, no. 1, pp. 150-155, Jan. 2008.
10. C.-Y. Chen, C.-Y. Hsu, and H.-T. Chuang, "Design of miniature planar dual-band filter using dual-feeding structures and embedded resonators," *IEEE Microwave and Wireless Component Letters*, vol. 16, no. 12, pp. 669-671, Dec. 2006.
11. M. Zhou, X. Tang, and F. Xiao, "Compact dual band bandpass filter using novel e-type resonators with controllable bandwidths," *IEEE Microwave and Wireless Components Letters*, vol. 18, no. 12, pp. 779-781, 2008.
12. Tsu-Wei, Lin, U-Hou, Lok, and Jen-Tasi, Kuo, "New dual mode dual-band bandpass filter with quasi-elliptic function passbands and controllable bandwidths," *Microwave Symposium Digest*, pp. 576-579, 2010.
13. M. -L. Chuang, M. -T. Wu, and S. -M. Tsai, "Dual-band filter design using L-shaped stepped impedance resonators," *IET Microwave Antennas Propagation*, vol. 4, Iss. 7, pp. 855-862, 2010.
14. He Zhu and Amin M. Abbosh, "Single- and Dual-Band Bandpass Filters Using Coupled Stepped-Impedance Resonators With Embedded Coupled-Lines," *IEEE MICROWAVE AND WIRELESS COMPONENTS LETTERS*, VOL. 26, NO. 9, SEPTEMBER 2016.
15. H. Zhu, E. Ahmed, and A. Abbosh, "Single- and dual-band bandpass filter using multi-mode resonator of short-ended and open ended coupled lines," in *Proc. Asia-Pacific Microw. Conf.*, Nanjing, China, Dec. 2015, pp. 1-3.
16. N. A. Wahab, M. K. M. Salleh, Z. I. Khan and Z. Awang, "Dual-Band Dual-Mode Bandpass Filter Using Series-Coupled Ring Resonators," 2012 IEEE Asia-Pacific Conference on Applied Electromagnetics (APACE 2012), December 11 - 13, 2012, Melaka, Malaysia.
17. Sha Luo and Lei Zhu, "A Novel Dual-Mode Dual-Band Bandpass Filter Based on a Single Ring Resonator," *IEEE MICROWAVE AND WIRELESS COMPONENTS LETTERS*, VOL. 19, NO. 8, AUGUST 2009.
18. Naoto Sekiya and Shunsuke Sugiyama, "Design of Miniaturized HTS Dual-Band Bandpass Filters Using Stub-Loaded Meander Line Resonators and Their Applications to Tri-Band Bandpass Filters," *IEEE TRANSACTIONS ON APPLIED*



-
- SUPERCONDUCTIVITY, VOL. 25, NO. 3, JUNE 2015.*
19. Y. T. Kuo, J. C. Lu, C. K. Liao, C. Y. Chang, "New multiband coupling matrix synthesis technique and its microstrip implementation," *IEEE Transactions on Microwave Theory and Techniques*, vol. 58, no. 7, pp. 1840-1850, July 2010.
20. Y. Nemoto, K. Kobayashi, and R. Sato, "Graphy transformations of nonuniform coupled transmission line networks and their application," *IEEE Trans. Microw. Theory Tech.*, vol. MTT-33, no. 11, pp. 1257-1263, Nov. 1985.
21. *EM User's Manual*, Sonnet Software, Inc., Syracuse, NY, USA, 2009. North